AUTHOR and OTHER-AUTHOR

[Left hand page running head is author's name in Times New Roman 8 point bold capitals, centred. For more than two authors, write **AUTHOR et al.**]

CONFERENCE PRE-PRINT

EFFECT OF DECREASING ASPECT RATIO ON ION-SCALE ELECTROSTATIC DRIFT-TYPE MODES AND PEDESTAL STABILITY IN H-MODE PLASMAS

J.Y. KIM Korea Institute of Fusion Energy Daejeon 34133, South Korea Email: jykim@kfe.re.kr

H.S. Han Korea Institute of Fusion Energy Daejeon 34133, South Korea

Abstract

As an effort to understand the H-mode property of the spherical tokamak (ST) with low aspect ratio (A), a modeling study is given on how the ion-scale electrostatic drift-type modes are linearly stabilized and how the pedestal stability varies when A decreases through major or minor radius. Firstly, for the electrostatic drift-type mode stabilization the following two mechanisms are newly identified to play an important role. One is the enhancement of the threshold temperature gradients for the ion temperature gradient mode (ITG) or trapped electron mode (TEM). The other is the increment of the ballooning force parameter α which roughly varies in proportion to $1/A^2$ when we assume a fixed safety-factor profile. This increment enhances the linear electromagnetic and Shafranov-shift effects, providing additional stabilization for the ITG and TEM, respectively. With this stabilization of the electrostatic drift-type modes, the electromagnetic kinetic ballooning mode (KBM) can be excited and a brief discussion is given for the way to improve further plasma confinement under such a situation. Meanwhile, in the case of the pedestal stability the eigenvalue spectrum of the peeling-ballooning mode (PBM) is first shown to have a complete shift to the n=1 limit when the elongation is very large (>2), as typically taken in the ST devices for maximizing its plasma performance. This shift makes the PBM stability sensitive to the edge safety-factor q(a), resulting in an oscillating behaviour of the threshold pedestal height (P_{ped}) when q(a) increases. It also allows the PBM to couple with the n=1 external kink mode when the normalized beta (β_N) approaches the no or ideal wall limit. When A decreases through the major or minor radius, these mode characteristics are maintained well, while Pped has a different behaviour depending on whether q(a) is fixed or varies with A. If plasma beta or β_N has a large increment through the toroidal field reduction with decreasing A, a sudden drop of P_{ped} is also shown to be possible by the excitation of the high-n ballooning-branch modes. Finally, a brief discussion is given about some discrepancies observed between the present ideal MHD modeling results and the experimental measurements in the contemporary ST devices.

1. INTRODUCTION

Spherical tokamak (ST) with a low aspect ratio (A) is receiving strong interest as a compact ignition device for economic fusion reactors. A particular feature of the ST is that the ion-scale electrostatic drift-type modes, such as the ion temperature gradient (ITG) or trapped electron mode (TEM), are often stabilized, with turbulent transport then dominated by the electron-scale mode or the electromagnetic modes, such as the kinetic ballooning mode (KBM) or micro-tearing mode (for example, see Ref.1-2). This change of the dominant turbulence mode is significant in that, in the conventional tokamak with high A, turbulent transport is typically governed by the ion-scale electrostatic modes so the suppression of such modes will facilitate the achievement of high beta plasma with improved confinement. It seems, however, still less certain how such a change or stabilization occurs, even though several mechanisms have been proposed. Closely related to this issue, it looks also important to check further how pedestal stability varies when tokamak type changes from the conventional to the ST one. This is since the overall performance of ST H-mode plasmas closely depends on pedestal height as well as core transport through the profile stiffness. As an effort to understand such global effects of the decreasing A, we here give a modelling study on the above two issues related to the core and pedestal regions, respectively.

2. ON THE STABILIZATION OF ION-SCALE ELECTROSTATIC DRIFT-TYPE MODES

For this study, we analyze the linear stability the ITG and TEM using some well-known analytic stability theory and kinetic simulation codes. For simplicity, most of these studies are conducted in the s- α equilibrium model. Even though this model becomes less accurate as A decreases, it can still provide useful information or insight as

long as *A* is not too low or near 1 (note that for the future ST devices, like STEP [3] or STAR [4], *A* has the design value of around 2 which is not so low). Meanwhile, to concentrate on the effects directly coming from decreasing *A* through the major radius (*R*) or minor radius (*a*), we here fix the safety-factor (*q*) and thus magnetic shear (*s*) profiles. Noting that in typical H-mode plasmas core density has a broad profile, we also mainly consider the ITG and the electron temperature gradient driven TEM (T-TEM), while a brief check also given on the density gradient driven TEM (D-TEM).

It is shown that, when A decreases, the linear stabilization of the ITG and TEM can occur through the following two new mechanisms [5]. One is the increase of threshold temperature gradient, which is particularly strong for the ITG and occurs clearly when A is reduced through R. To see this, note first that in the broad density profile condition the threshold ion temperature gradient roughly has the form, $\left(\frac{R}{L_{Ti}}\right)_c \simeq 2(1+\tau)$ for the ITG, while $\left(\frac{R}{L_{Te}}\right)_c \simeq \frac{2}{f_t} \left(1 + \frac{1}{\tau}\right)$ for the T-TEM, where $\tau = T_i/T_e$ and $f_t \sim \left(\frac{2\varepsilon}{1+\varepsilon}\right)^{1/2}$ with $\varepsilon = r/R$ (see Ref. 5-6 for the detailed derivation of them). These forms show clearly that the threshold temperature gradients become smaller $[(L_{Ti})_c \propto R \text{ and } (L_{Te})_c \propto R^{1/2}]$ so the marginal temperature profiles become steeper as R decreases. To check these analytic results we have also performed numerical calculations using the local kinetic code [7]. As shown in Fig. 1, the threshold temperature gradients for the ITG and T-TEM (and also the threshold density gradient for the D-TEM) have substantial enhancement when R decrease from 1.8 \rightarrow 0.9m, in qualitative agreements with the above analytic estimates. These increases of the threshold gradients are mainly attributed to the enhancement of magnetic curvature drift resonance with decreasing R. When A decreases through a, unlike the above decreasing R case there is no change in the actual threshold temperature gradient. However, the effective one defined in terms of the normalized minor radius still has an increase, resulting in similar enhancement of core temperature at the plasma center. The other important stabilization by the decreasing A arises through the increment of the ballooning force parameter α , which is found to roughly vary in proportion to $1/A^2$ when we assume a fixed q-profile (see also Ref. 5 for more details). This increase of α then enhances the linear electromagnetic and Shafranov-shift effects, which are known to give a strong stabilization on the ITG and TEM, respectively.

While the ion-sale electrostatic drift-type modes are thus expected to be strongly stabilized in the ST devices with low A, a problem can still arise from the excitation of the electromagnetic KBM. In fact, with the increment of α , the standard KBM is excited at a smaller pressure gradient, thus preventing an appreciable confinement improvement. Fortunately, in the ST devices where elongation is typically very large, plasma can have the 2^{nd} stability regime access over most core region. Even in this case, however, a new type of the KBM or the hybrid KBM may be excited, as shown in the recent simulation work of the target scenario of the STEP by Kennedy et al. [2]. It is still less clear how this destabilization of the hybrid KBM is possible. In Ref. 2, it was initially suggested that the destabilization may be due to the effect of the parallel magnetic perturbation (δB_{\parallel}) of which the magnitude typically increases with plasma beta, but in the subsequent work it was shown to be also possible even without such an effect. Meanwhile, the fact that the hybrid-KBM is a mixture of the KBM and TEM with the

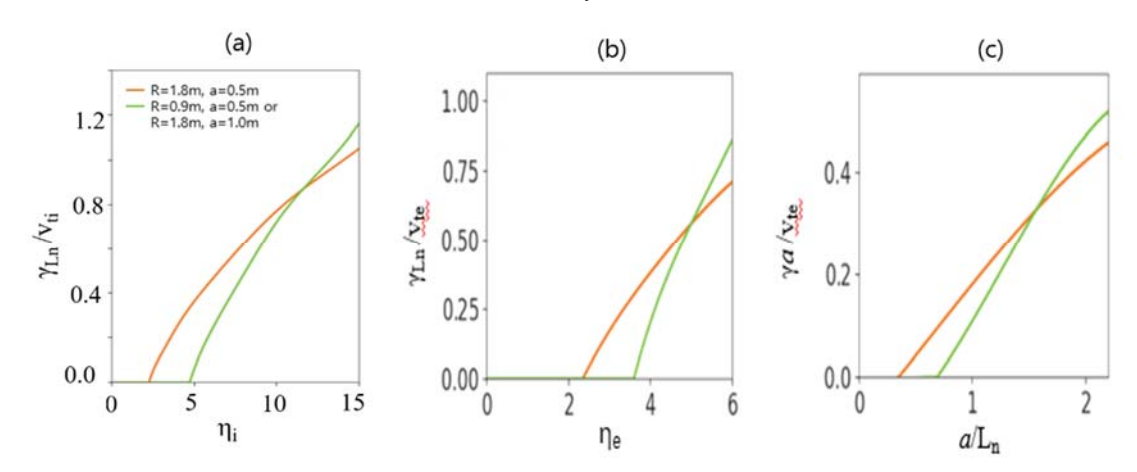


FIG. 1. Variation in the normalized growth rate as a function of temperature or density gradient when A=R/a decrease from 3.6 to 1.8 through $R=1.8\rightarrow0.9$ m or $a=0.5\rightarrow1.0$ m. Note that (a), (b), (c) represent the ITG, T-TEM, D-TEM cases, respectively, with $\eta_i=L_n/L_{Ti}$ and $\eta_i=L_n/L_{Te}$ when $\tau=1$, $k_y=0.5$ and $L_n=0.9$ m [in (a) and (b)].

[Left hand page running head is author's name in Times New Roman 8 point bold capitals, centred. For more than two authors, write AUTHOR et al.]

destabilization enhanced when the q-value decreases or the s-value increases suggests that it may be closely related to the weakening of the Shafranov-shift effect. While this latter effect is usually known to give a stabilization on the KBM and TEM, some weakening may occur through the enhanced δB_{\parallel} . Note also that the reduction of the Shafranov-shift stabilization may occur by the high β_T effect which is newly found to give a destabilization on the ballooning-type mode, as will be more discussed in Sec. 3.

Finally, based on the present modelling results and the above consideration on the KBM, it may be worthwhile to give here an overall picture of how the stability properties of the electrostatic and electromagnetic modes vary when A decreases and thus α increases. Figure 2 shows a schematic diagram for illustrating such a picture. Note first that in the conventional tokamak with high A, the temperature gradient is typically constrained by the electrostatic ITG, making plasma β and α stay in the relatively low value range, roughly, at the point slightly above $\alpha_{\rm ITG,1}$ in Fig. 2. As A decreases and thus α approaches $\alpha_{\rm ITG,2}$ the ITG is completely stabilized by the linear electromagnetic effect. With this stabilization of the ITG, the temperature gradient or α will increase further until it encounters the TEM excitation at the point of $\alpha_{\text{TEM},1}$ (in the dashed line with R=0.9m and $q=q_1$). Of course, before to reach such a point the standard KBM can be excited around $\alpha_{ITG,2}$, but this mode is expected to have the 2nd stability regime access if plasma shaping is strong and magnetic shear is not so large. A key question is then how much the Shafranov-shift effect is strong to stabilize the TEM at the point around $\alpha_{TEM,1}$. Clearly, this will depend on how much $\alpha_{TEM,1}$ is close to $\alpha_{TEM,2}$. Apparently, there are three ways to make such a gap close or disappear. The first is to increase $\alpha_{\text{TEM},1}$ directly through the q-value increment (at a fixed temperature gradient), as illustrated by the dotted line in Fig. 2 (recall that $\alpha_{\text{TEM},2}$ mainly depends on s so almost independent of such a q-value change). The second is to increase $\alpha_{\text{TEM},1}$ through the enhancement of the TEM threshold temperature gradient itself, for example, by stronger plasma shape. The last is to decrease $\alpha_{\text{TEM},2}$ through the enhancement of the Shafranov-shift effect, for example, by weaker magnetic shear. Here, one thing to note is that the hybrid-KBM may also be excited when A decreases and α increases, as discussed above. While this mode is observed to be restabilized as a becomes high (as expected from the Shafranov-shift effect), it is still less clear how this mode is excited or what is the threshold for its excitation. The fact that this mode is a mixture of the TEM and KBM suggests that there may be some correlation in the excitation threshold between the hybrid-KBM and the pure-TEM. To reach the high β or α regime, it will be important to minimize the gap between the excitation and stabilization thresholds of the hybrid-KBM, so it may be worthwhile to check whether the methods proposed above for the pure-TEM can be also applied to the hybrid-KBM case.

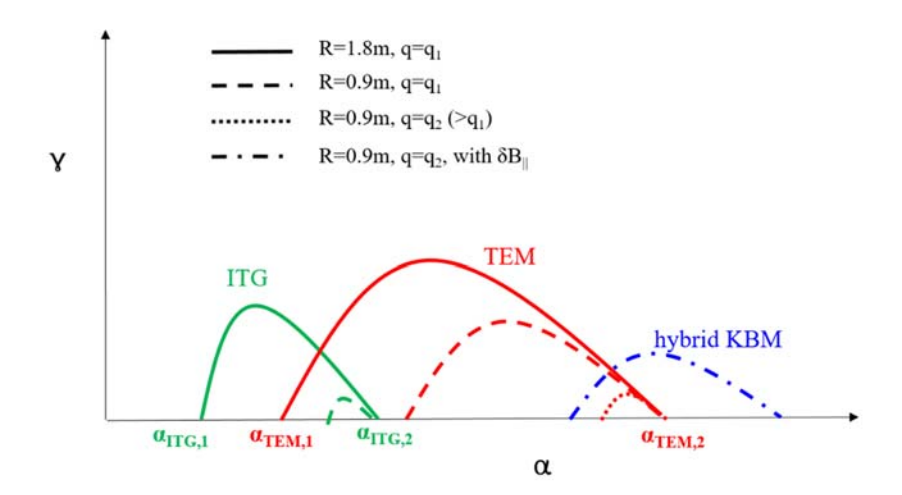


FIG. 2. A schematic diagram illustrating the variation of the stability properties of the ITG, TEM and KBM when α increases, with the possible effects of the decreasing R and the increasing q-value. Here, $\alpha_{\text{ITG},1}$ and $\alpha_{\text{ITG},2}$ ($\alpha_{\text{TEM},1}$ and $\alpha_{\text{TEM},2}$) are the α values at the points where the ITG (TEM) are excited and stabilized by the linear electromagnetic (Shafranov-shift) effect, respectively.

ON THE PEDESTAL STABILITY VARIATION

For the study of this issue, we here use the well-known HELENA-MISHKA1 code package. Noting that the ST devices typically have a very large elongation (for example, with $\kappa=3$ in STEP [3]) to utilize its inherent stability against the vertical instability, the present study is mainly focused on such a strong shape plasma. With the usual high sensitivity of pedestal stability to the edge safety-factor q(a), the two cases are also considered where q(a) is fixed or allowed to vary when R or a changes. We first consider the pedestal stability in the very large κ regime, and then check how it varies when A decreases through R or a.

Figure 3 shows the calculation results of the pedestal stability variation when κ increases up to 3. Note that these calculations were done in the reference equilibrium (with R=1.8m, a=0.5m, $B_T=2.0T$, and $\delta=0.5$), with the other parameters assumed to have the values of $q(a)\sim 5$ and $\beta_P\sim 1.0$, where β_P is the poloidal plasma beta. From Fig. 3, we can first see that the increasing κ induces a significant increment of the threshold pedestal height (P_{ped}), with the shift of the peak-n number to the low-n regime. While this result is similar to that shown in our previous work [8], it is now seen that, with a further increase of κ above 2, the peak-n number has a complete shift to the n=1 limit. Notably, this shift occurs even when we normalize the growth rate (γ) by the Alfven frequency (ω_A), instead of $\omega_{*pi}/2$ which is usually used to get P_{ped} with the criterion of $\gamma/(\omega_{*pi}/2)\sim 1$ (here, ω_{*pi} is the half maximum of the ion diamagnetic drift frequency across the pedestal). In the case of Fig. 3(a), the threshold κ for the complete transition to n=1 (in terms of the growth rate normalized by $\omega_{*pi}/2$) is found to be about 2.0. We have checked how this threshold κ depends on the other parameters, like δ , q(a) and β_P , finding that in such cases the dependences are relatively weak, with a small reduction when δ becomes lower or q(a) and β_P higher than the above reference values. As will be shown later, this weak dependence also applies for A, with the threshold κ being slowly reduced as A decreases.

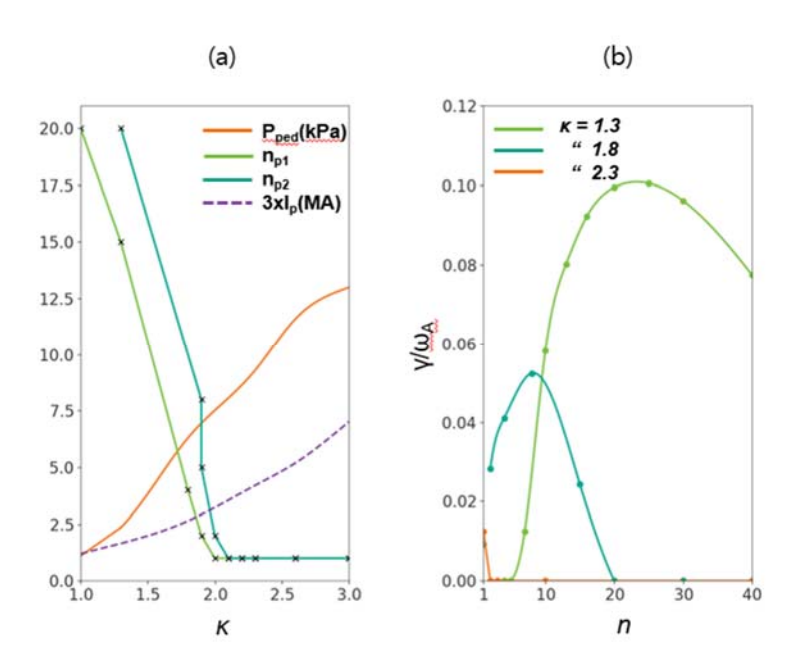


FIG. 3. (a) P_{ped} , peak *n*-numbers and I_P as a function of κ when $q(a)\sim5.0$, $β_P\sim1.0$ and $\Delta_{\psi}\sim0.04$ in the conventional tokamak model with R=1.8m, a=0.5m, $B_T=2.0$ T and $\delta=0.5$. Here, n_{p1} and n_{p2} represent the peak-n numbers of the growth rate normalized by the Alfven (ω_A) and ion diamagnetic drift ($\omega_{*pi}/2$) frequencies, respectively. For comparison, also shown are (b) the eigenvalue spectrums at $\kappa=1.3$, 1.8, and 2.3.

A natural consequence of the shift of the PBM eigenvalue spectrum to the strongly peeling-dominant regime is that the pedestal stability becomes sensitive to the distance between the last closed flux-surface and the adjacent outer rational surface, as is known well for the peeling-type mode [9]. Since this distance has a periodic variation when q(a) increases, an oscillating behaviour can then occur in the pedestal stability or P_{ped} . Here, one thing to note is that in the strong shape plasma the local q-value has a non-negligible variation along the field line so there can exist multiple resonant harmonics on the last closed flux-surface. Using the HELENA-MISHKA code package, we now check how P_{ped} then depends on the flux-surface averaged q(a). Figure 4 shows the calculation result at κ =2.3, which is well above the threshold κ for the n=1 shift. For comparison, also shown is the result at κ =1.3, where the peak-n number is about 20, so it is in the ballooning-dominant regime. From Fig. 4(a) we can first see that in the peeling-dominant regime of κ =2.3 P_{ped} has a sensitive dependence on q(a) with a clear

[Left hand page running head is author's name in Times New Roman 8 point bold capitals, centred. For more than two authors, write AUTHOR et al.]

oscillating behaviour. This is well contrasted to the high-n ballooning-dominant case of κ =1.3 in Fig. 4(b) where such an oscillation almost disappears. From Fig. 4(a) we can also see that the oscillation peaks at the points where q(a) has an integer value, in qualitative agreement with the observed feature in Ref. 9. Besides the above, we also note that, with the shift to the n=1 limit, the PBM can couple to the n=1 external kink mode as the normalized beta (β_N) approaches the no or ideal wall limit, as also observed in the high poloidal-beta discharge case [10].

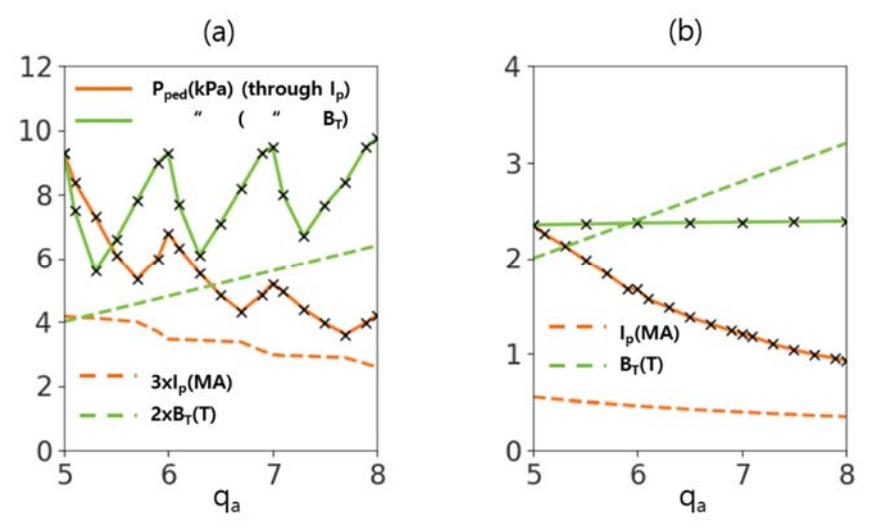


FIG. 4. Variation of P_{ped} when q(a) increases through I_P (at a fixed B_T~2.0T) or B_T (at a fixed I_P~1.4MA) in the two cases of (a) $\kappa=2.3$ and (b) $\kappa=1.3$ with the other parameters the same as Fig. 1.

In the above, we have studied the pedestal stability of the plasma with a very large κ in the conventional tokamak model with high A. Here, we now check how such a pedestal stability varies when A decreases. Figure 5 shows the calculation results of the pedestal stability change when R decreases from 1.8m to 0.9m at a=0.5m (so A decreases from 3.6 to 1.8), with q(a) fixed to 5.0. Even though not shown in Fig. 5, note first that there is no change in the peak-n number, with the n=1 mode still dominant when R decreases. More specifically, we find that the threshold κ for the n=1 shift has a small reduction from about 2.0 to 1.8 when R decreases from 1.8m to 0.9m. From Fig. 5, we then note that there is a non-negligible increment of P_{ped} when R decreases. Considering that we have here fixed q(a), this increment is somewhat unexpected one. Some explanation may, however, be found if we note that there is a modest increase of I_P even when q(a) is fixed and B_T is reduced with R. It is easy to see that this increase of I_P occurs since, when R and thus A decreases, the local B_T has a more rapid variation on a given flux surface, with a larger difference between the inboard and outboard sides. To have the same flux-surface averaged q(a) value, I_P should then increase with decreasing R or A. Note that this is indeed the reason why the

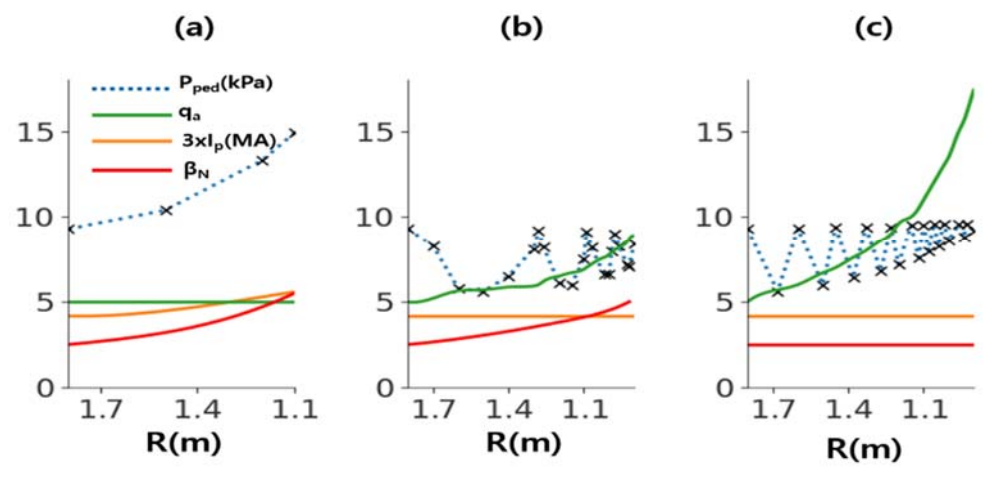


FIG. 5. Variation in various plasma parameters, including P_{ped} , when R decreases at a fixed a(=0.5m) in the three cases where (a) q(a) is fixed to 5.0 or (b) I_P is fixed to 1.4MA with $B_T \propto R$, and (c) I_P and B_T are fixed to 1.4MA and 2.0T, respectively. Plasma elongation and triangularity are assumed to be κ =2.3 and δ =0.5, with poloidal plasma beta of β P~1.0 in most cases.

ST is often called the 'high-current' device [1]. If we recall that the dependence of P_{ped} on q(a) mainly comes through I_P , this increase of I_P may then explain how P_{ped} can have a non-negligible increment when R decreases.

The other notable feature from Fig. 5 is that P_{ped} has a different behaviour, depending on whether q(a) is fixed or not. When q(a) is fixed, P_{ped} has a non-negligible increment with decreasing R or A, as shown above. Meanwhile, when I_P is fixed so q(a) varies with A, P_{ped} has no more increase but takes an oscillation. This behaviour may be understood well if we note that, even with the fixed I_P , q(a) has a modest increase when R decreases, mainly due to the enhanced toroidicity effect mentioned earlier. Similar to Fig. 4, P_{ped} can then have an oscillating behaviour with its peaks at the integer q(a) points while the peak amplitude being almost the same with the constant I_P . To check this further, we have also considered the case where B_T has no more reduction when R decreases. Figure S(c) shows the calculation results when S(c) is fixed to 2.0T with S(c) with S(c) have that S(c) now has a more rapid increment with decreasing S(c), with the corresponding large increase of the oscillation frequency.

The other interesting feature observed from the present study is that, as shown in Fig. 6(a), there can be a sudden drop of P_{ped} when R becomes smaller than a threshold, roughly about 1.1m at β_{P} ~1.0. From the eigenvalue spectrum of the PBM, this drop is found to be due to the excitation of the high-n ballooning branch modes at a smaller P_{ped} . As shown in Fig. 6(b), however, these modes appear to have the eigenmode structure which is peaked in the inner core region inside the pedestal, different from the typical PBM ones peaked near the boundary. To find the physics origin of them, we have performed a local stability analysis of the infinite-n ballooning mode using the module in the HELENA code. Figure 6(c) shows the calculation results at various R cases (with the pedestal height roughly assumed as about 10kPa in most cases). Note here that each line indicates the trajectory in the s- α domain when one moves from the core to edge, with the ballooning unstable radial points denoted by 'x'. It is seen that, as R decreases, the infinite-n ballooning mode starts to be excited from the inner core region, with the unstable zone being then expanded outward. The unstable zone reaches the pedestal (which is here the region where α has a rapid increase with the reduction of s) at around $R \sim 1.1$ m where the high-n branch modes are excited. This result thus indicates that the excitation of the high-n branch modes is closely related to the destabilization of the infinite-n ballooning modes and its expansion to the pedestal. Here, one question may arise of how the infinite-n ballooning modes can be destabilized in the present very large κ regime where they are expected to have the 2^{nd} stability transition. To answer this, we have checked the other cases where β_P is reduced or B_T increases. We then find that the excitation of the infinite-n ballooning or high-n branch modes are delayed or disappear. From a separate study [11] we indeed find that the destabilization of the infinite-n ballooning modes is mainly due to the toroidal plasma beta (β_T) , which is substantially enhanced when B_T is reduced with R or A in the ST devices.

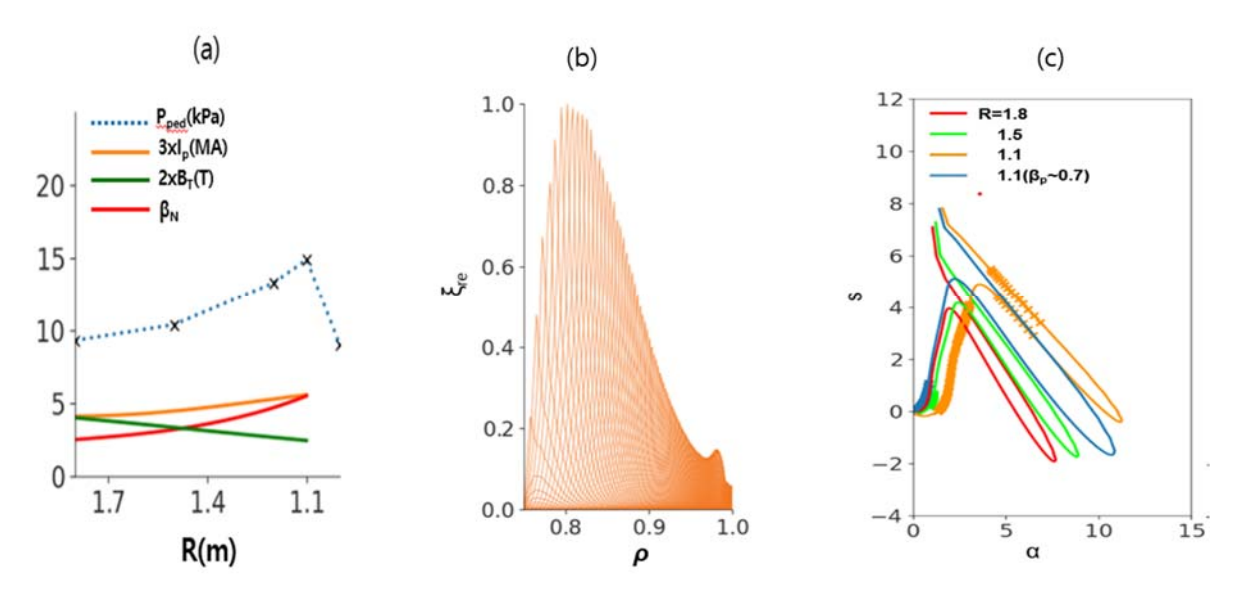


FIG. 6. (a) Sudden drop of P_{ped} when R decreases below a threshold (~1.1m) by the excitation of the high-n ballooning branch mode with (b) the mode structure. Also shown is (c) the variation in the unstable points of the infinite-n ballooning modes along the equilibrium trajectories in the s-alpha domain when R decreases. Here, q(a) is fixed to 5.0 with $B_T \propto R$, and κ =2.3, δ =0.5 and $\beta_P \sim$ 1.0.

[Left hand page running head is author's name in Times New Roman 8 point bold capitals, centred. For more than two authors, write

AUTHOR et al.]

Finally, we here discuss briefly some discrepancies observed between the present modelling results based on the ideal MHD and the experimental measurements in the contemporary ST devices. Note first that, while the present study predicts the dominance of the n=1 mode with the relatively high P_{ped} values, many experimental measurements in MAST and NSTX show the ELM structure dominated by the intermediate or high-n modes with the measured P_{ped} also substantially smaller than the above modelling one (for example, see Ref. 12-13). This mismatch in the dominant mode number or P_{ped} was indeed already recognized in some previous works. For example, earlier analyses of the MAST discharges [12] showed that there is no unstable ballooning-type mode over the range of 6 < n < 50 or the PBM eigenvalue spectrum peaks in the very low-n regime (~ 3). A similar result was also obtained from the recent analyses of the NSTX discharges [14] where experimental pedestal profiles are found to be well below the stability boundary of the intermediate-n modes when analysed by using the ELITE code. Here, we now discuss some models which may provide a clue to resolve such a discrepancy. The first is the resistivity effect. The above analysis work of the NSTX discharges [14] indeed shows that the intermediate-n modes can be unstable if the discharges are analysed by using the M3D-C1 code which includes the resistivity effect. The second is the enhanced kinetic effect. This possibility is suggested from the recent work by J. F. Parisi et al. [15] which shows that, with the enhanced destabilization of the KBM far below the ideal threshold, it is possible to explain the wide pedestal width scaling observed in NSTX [16]. Even though this work mostly concerns the mismatch observed in the pedestal width between the modeling and experiments it may also provide a clue for resolving the above issue about P_{ped} because, in destabilizing the ideal ballooning mode, the kinetic effect is expected to play a similar role as the resistivity. Finally, the generation of the intermediate-n modes may also be facilitated by the high β_T effect shown in the present work. As described earlier, this effect can destabilize the high-n ballooning-branch modes around the pedestal, inducing a substantial drop of P_{ped}. It is also possible to facilitate the intermediate-n mode generation through a synergy process. For example, with the resistivity and high β_T effects primarily working near the pedestal foot (where the temperature is low) and the pedestal top/center, respectively, their coupling can enhance the destabilizing force for the intermediate-n mode generation over the pedestal region (see Ref. 17 for a more detailed discussion on all of the above points).

ACKNOWLEDGEMENTS

This work was supported by the Ministry of Science and ICT of Korea under the KFE (Korea Institute of Fusion Energy) R&D Program of KSTAR Experimental Collaboration and Fusion Plasma Research (KFE-EN2301).

REFERENCES

- [1] KAYE S. M. et al., Plasma Phys. Control. Fusion 63, 123001 (2021).
- [2] KENNEDY D. et al., Nucl. Fusion 63, 126061 (2023) and Nucl. Fusion 64, 086049 (2024).
- [3] THORELUS E. et al., Nucl. Fusion 64, 106030 (2024).
- [4] BROWN T.G. and MENARD J.E., Fusion Engineering and Design 192, 113583 (2023).
- [5] KIM J.Y. et al., Nucl. Fusion **65**, 036019 (2025).
- [6] ROMANELLI F., Phys. Fluids B 1, 1018 (1989).
- [7] KIM J.Y. et al., Nucl. Fusion **59**, 056021 (2019).
- [8] KIM J.Y. et al., Phys. Plasmas **30**, 050702 (2023).
- [9] CONNOR C.W. et al., Phys. Plasmas 5, 2687 (1998).
- [10] GAROFALO A. M. et al., Nucl. Fusion 55, 123025 (2015).
- [11] KIM J.Y. et al., to be submitted to Phys. Plasmas.
- [12] KIRK A. et al., Plasma Phys. Control. Fusion 47, 315 (2005).
- [13] IMADA K. et al., Nucl. Fusion 64, 086002 (2024).
- [14] KLEINER A. et al., Nucl. Fusion 61, 064002 (2021).
- [15] PARISI J.F. et al., Nucl. Fusion 64, 054002 (2024).
- [16] DIALLO A. et al., Nucl. Fusion 53, 093026 (2013).
- [17] KIM J.Y. et al., 2025 Nucl. Fusion https://doi.org/10.1088/1741-4326/ae0cdc.